Letter

Low-Power Switching of Magnetization Using Enhanced Magnetic Anisotropy with Application of a Short Voltage Pulse

R. Matsumoto* and H. Imamura†

National Institute of Advanced Industrial Science and Technology (AIST), Spintronics Research Center, Tsukuba, Ibaraki 305-8568, Japan

(Received 8 January 2020; revised 28 July 2020; accepted 14 August 2020; published 31 August 2020)

A low-power magnetization-switching scheme based on the voltage control of magnetic anisotropy is proposed. In contrast to the conventional switching scheme using voltage control of magnetic anisotropy, where the magnetic anisotropy is eliminated during the voltage pulse, in the proposed scheme the magnetic anisotropy is enhanced to induce precession around the axis close to the easy axis. After the voltage is turned off at approximately half the precession period, the magnetization relaxes to the opposite equilibrium direction. We perform numerical simulations and show that the pulse duration of the proposed switching scheme is as short as a few tens of picoseconds. Such a short pulse duration is beneficial for low-power consumption because of the reduction of energy loss by Joule heating.

DOI: 10.1103/PhysRevApplied.14.021003

Low-power consumption is a key requirement for modern computational devices. Nonvolatility is one of the core concepts to reduce power consumption for logics and memories in normally-*off* computing [1–3]. Magnetoresistive random-access memory (MRAM) is a promising nonvolatile memory that stores information associated with the direction of magnetization in magnetic tunnel junctions (MTJs) [4–12]. To reduce power consumption of MRAM, several types of writing schemes have been developed. The currently used writing scheme is based on the spin-transfer-torque (STT) switching phenomena, which were independently proposed by Slonzewski [13,14] and Berger [15]. The write energy of STT MRAM is on the order of 100 fJ/bit [9,12], which is still 2 orders of magnitude larger than that of static random-access memory.

Discovery of the voltage-control-of-magnetic-anisotropy (VCMA) effect [16–26] paved the way for further reduction of write energy in MRAM. The mechanism of VCMA in a MgO-based MTJ is considered to be the combination of the selective electron or hole doping in the *d*-electron orbitals and the induction of a magnetic dipole moment, which affect the electron spin through spin-orbit interaction [18–20,27]. The MRAM that uses the VCMA effect to switch magnetization is called the "voltage-controlled MRAM" (VCMRAM) [28–40]. The writing procedure for a conventional VCMRAM is as follows. The perpendicularly magnetized MTJ is subjected to an in-plane external magnetic field ($H_{\rm ext}$) as shown in Fig. 1(a). The magnetic anisotropy constant of the free layer can be controlled by applying a voltage (V) as shown in Fig. 1(b), where, $K_{\rm eff}$ is the effective perpendicular anisotropy constant, where the demagnetization energy is subtracted from the perpendicular anisotropy constant. Throughout the letter, the superscript (0) indicates the quantities at $V = 0$. The voltage pulse with critical amplitude V_c eliminates the magnetic anisotropy and induces the precession of the magnetization around the external magnetic field. If the voltage is turned off at half the precession period, the magnetization switching is completed.

The write energy of VCMRAM is estimated from the Joule-heating energy loss during the pulse. Assuming that a voltage pulse with amplitude V and duration t_p is applied to the MTJ with resistance R, the write energy is given by

$$E_J = \frac{V^2}{R} t_p. \tag{1}$$

To reduce the write energy, the VCMRAM should be designed to have large resistance and short pulse duration. The pulse duration is given by half the precession period as

$$t_p = \frac{\pi(1+\alpha^2)}{\gamma H_{\rm ext}}, \tag{2}$$

where α is the Gilbert damping constant and γ is the gyromagnetic ratio. For example, $t_p = 0.18$ ns for $\alpha = 0.1$ and $\mu_0 H_{\rm ext} = 100$ mT, where μ_0 is the vacuum permeability. Recently, Grezes *et al.* [32] demonstrated a very small write energy of 6 fJ/bit for a VCMRAM with $R = 330$ kΩ at $V = 1.96$ V and $t_p = 0.52$ ns. Similar results were obtained independently by Kanai *et al.* [33].

*rie-matsumoto@aist.go.jp
†h-imamura@aist.go.jp

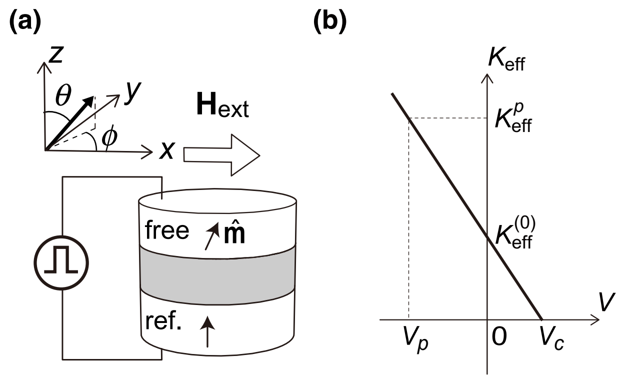

FIG. 1. (a) Magnetic tunnel junction with a circular cylinder shape, and definitions of Cartesian coordinates (x,y,z), polar angle (θ), and azimuthal angle (ϕ). The x axis is parallel to the direction of the external in-plane magnetic field, $\mathbf{H}_{\rm ext}$. The unit vector $\hat{\mathbf{m}}=(m_x,m_y,m_z)$ represents the direction of the magnetization in the free layer. The magnetization in the reference layer (ref.) is fixed for alignment in the positive z direction. (b) The voltage (V) dependence of the effective perpendicular anisotropy constant $(K_{\rm eff})$. The effective anisotropy constant at $V=0$ is represented by $K_{\rm eff}^{(0)}$. $K_{\rm eff}=K_{\rm eff}^{p}$ at $V=V_p$.

It is difficult to use a MTJ with huge R to further reduce the write energy because the read time of the VCMRAM increases with increase of R. Use of a scheme for decreasing the pulse duration by increasing the external magnetic field should also be avoided since the application of a strong in-plane magnetic field $H_{\rm ext}$ reduces the thermal-stability factor defined as [31]

$$\Delta^{(0)}=\frac{\mu_0 H_K^{(0)} M_s V_F}{2k_B T}\left(1-\frac{H_{\rm ext}}{H_K^{(0)}}\right)^2, \tag{3}$$

where k_B is the Boltzmann constant, T is the temperature, M_s is the saturation magnetization, V_F is the volume of the free layer, and $H_K^{(0)}[=2K_{\rm eff}^{(0)}/(\mu_0 M_s)]$ is the effective perpendicular anisotropy field.

In this letter, we propose another switching scheme that could reduce the pulse duration and therefore the write energy of a VCMRAM. The main difference between the conventional scheme and the proposed switching scheme is the polarity of the voltage pulse. Application of the voltage pulse with polarity opposite that in the conventional switching can enhance the magnetic anisotropy and induce precession around the axis close to the easy axis. After the voltage is turned off at approximately half the precession period, the magnetization relaxes to the opposite equilibrium direction and the switching is completed. We perform numerical simulations and demonstrate that the pulse duration of the proposed switching scheme is as short as a few tens of picoseconds. We also evaluate the write error rate (WER) and show that the WER is minimized if the pulse duration is about half the precession period, which is similar to the conventional switching scheme.

The system we consider is shown schematically in Fig. 1(a). The macrospin model is used to describe the magnetization dynamics. The direction of the magnetization in the free layer is represented by the unit vector $\hat{\mathbf{m}}=(m_x,m_y,m_z)=(\sin\theta\cos\phi,\sin\theta\sin\phi,\cos\theta)$, where θ and ϕ are the polar and azimuthal angles. The x axis is parallel to the direction of the external in-plane magnetic field $\mathbf{H}_{\rm ext}$.

The energy density of the free layer is given by

$$\mathcal{E}(m_x,m_y,m_z)=-K_{\rm eff}m_z^2-\mu_0 M_s H_{\rm ext} m_x. \tag{4}$$

The first term in Eq. (4) is the sum of the shape, the bulk crystalline, and the interfacial anisotropies. Owing to the VCMA effect, $K_{\rm eff}$ can be controlled by application of a voltage as shown in Fig. 1(b), where $K_{\rm eff}^{(0)}$ represents the effective anisotropy constant without the voltage application. We assume that $K_{\rm eff}$ decreases with increase of V and vanishes at $V=V_c$. Application of the voltage $V_p(<0)$ increases $K_{\rm eff}$ to $K_{\rm eff}^{p}$ and induces the precessional motion of $\hat{\mathbf{m}}$ around the effective magnetic field. The effective field $H_{\rm eff}=(H_{\rm ext},0,H_K m_z)$, where $H_K=2K_{\rm eff}^{p}/(\mu_0 M_s)$ is the anisotropy field.

The magnetization dynamics is simulated by our solving the following Landau-Lifshitz-Gilbert equation: [41],

$$\frac{d\hat{\mathbf{m}}}{dt}=-\gamma_0\hat{\mathbf{m}}\times(\mathbf{H}_{\rm eff}+\mathbf{h})+\alpha\hat{\mathbf{m}}\times\frac{d\hat{\mathbf{m}}}{dt}, \tag{5}$$

where $\mathbf{h}$ represents the thermal-agitation field satisfying the relations

$$\langle h_\iota(t)\rangle=0 \tag{6}$$

$$\langle h_\iota(t)h_\kappa(t')\rangle=\frac{2\alpha k_B T}{\gamma_0\mu_0 M_s V_F}\delta_{\iota\kappa}\delta(t-t'), \tag{7}$$

where $\iota,\kappa=x,y,z$, and $\langle X\rangle$ denotes the statistical average of X.

Throughout this letter, we assume that the external field $\mu_0 H_{\rm ext}=100$ mT and the saturation magnetization of the free layer $M_s=1400$ kA/m. Also we assume the radius r of the junction area to be 50 nm and the thickness of the free layer $t_F=1$ nm, and therefore the volume of the free layer $V_F=\pi r^2 t_F=7854$ nm^3. The initial states are prepared by 10-ns relaxation from the equilibrium direction at $K_{\rm eff}^{(0)}=100$ kJ/m^3 and $T=0$; that is, $(\theta^{(0)},\phi^{(0)})=\{\sin^{-1}[\mu_0 M_s H_{\rm ext}/(2K_{\rm eff}^{(0)})],0\}$ [38]. The write error rates are calculated from 10^6 trials with 10-ns relaxation after the pulse.

First we show the difference between the mechanisms of the conventional voltage-controlled switching and the proposed switching that uses the enhancement of the magnetic

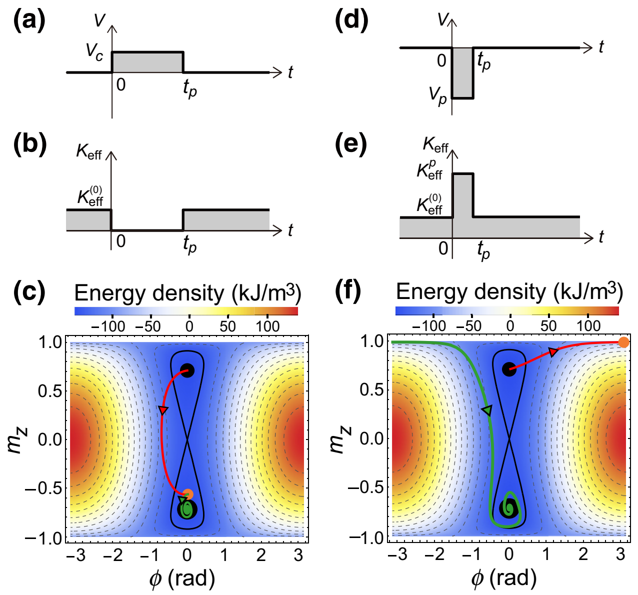

FIG. 2. (a) The shape of the voltage pulse for the conventional switching scheme. The amplitude including the polarity of the pulse and the duration of the pulse are V_c (positive value) and t_p, respectively. (b) The corresponding time dependence of the effective anisotropy constant $K_{\rm eff}$. At $V = 0$, it takes the value $K_{\rm eff}^{(0)}$. During the pulse, $K_{\rm eff} = 0$ because $V = V_c$. (c) The color map of the energy density at $V = 0$ on the ϕ-m_z plane. Thin dotted black curves represent energy contours. Thick black curves represent the energy contour crossing $\hat{\mathbf{m}} = (1, 0, 0)$. The trajectories of $\hat{\mathbf{m}}$ during and after the pulse are shown by the red and green curves, respectively. The direction of the trajectory is indicated by the triangle. The orange circle represents the direction of $\hat{\mathbf{m}}$ at the end of the pulse. We assume that $\alpha = 0.1$. (d) The shape of the voltage pulse for the proposed switching scheme. The polarity is negative (i.e., $V_p < 0$) to increase $K_{\rm eff}$. (e) The corresponding time dependence of the effective anisotropy constant. During the pulse, it is increased to $K_{\rm eff}^p$. (f) The color map of the energy density at $V = 0$ on the ϕ-m_z plane. We assume that $K_{\rm eff}^p = 400$ kJ/m^3 and $\alpha = 0.21$. The symbols are the same as those in (c). The left and right boundaries at $\phi = \pm\pi$ represent the same direction of $\hat{\mathbf{m}}$.

anisotropy. This is accomplished by our analyzing the switching trajectories at $T = 0$. Figures 2(a) and 2(b) show the shape of the voltage pulse and the corresponding time dependence of the effective anisotropy constant for the conventional voltage-controlled switching. The induced switching dynamics of $\hat{\mathbf{m}}$ at $T = 0$ is shown in Fig. 2(c) together with the color map of the energy density of Eq. (4) at $V = 0$. Thin dotted black curves represent energy contours. Thick black curves represent the energy contour crossing $\hat{\mathbf{m}} = (1, 0, 0)$. The initial direction of the magnetization is the equilibrium direction with $m_z > 0$ indicated by the black circle, which we call the "up state."

In Figs. 2(a)–2(c), application of a voltage pulse with V_c eliminates the magnetic anisotropy and induces the precession of $\hat{\mathbf{m}}$ around the external magnetic field as represented by the red curve. After the voltage is turned off at half the precession period, the magnetization starts to relax from the point indicated by the orange circle to the other equilibrium direction with $m_z < 0$ (i.e., the "down state"), indicated by the black circle. Note that the black circle at $m_z < 0$ is illustrated under the green curve. The switching is thus completed as represented by the green curve.

Figures 2(d) and 2(e) show the shape of the voltage pulse and the corresponding time dependence of the effective anisotropy constant for the switching using the increased $K_{\rm eff}$. The induced switching dynamics of $\hat{\mathbf{m}}$ at $T = 0$ is shown in Fig. 2(f) together with the color map of the energy density at $V = 0$. The initial state is the up state indicated by the black circle at $m_z > 0$. Application of a voltage pulse with $V_p(< 0)$ increases the effective anisotropy constant from $K_{\rm eff}^{(0)}$ to $K_{\rm eff}^p$ and induces precession of $\hat{\mathbf{m}}$ around the effective magnetic field as represented by the red curve. The value of $K_{\rm eff}^p$ is assumed to be 400 kJ/m^3, which gives an anisotropy field of $\mu_0 H_K = 570$ mT. The effective field is nearly parallel to the easy axis or the z axis because the directional cosine of the effective field relative to the easy axis is 0.98. The voltage is turned off at about a half the precession period, and the magnetization reaches the point $\phi \simeq \pi$ indicated by the orange circle. As shown later, WER is minimized if the pulse duration is set to about half the precession period. After the pulse is turned off, the magnetization relaxes to the down state and completes the switching as shown by the green curve. The proposed switching scheme does not reduce the thermal-stability factor in Eq. (3) because it increases $K_{\rm eff}$ during the voltage pulse.

To check the stability of the proposed writing scheme, we conduct micromagnetic simulations on the basis of the simulation parameters in Fig. 2(f) with use of the software package MuMax3 [42]. Even for an exchange stiffness constant ($A_{\rm ex}$) of 2×10^{-11} J/m and bias current density (J) of $|J| = 10^{13}$ A/m^2, which induces the Oersted field ($H_{\rm Oe}$) ranging from 0 (at the center of the cylinder) to $\mu_0 H_{\rm Oe} = 314$ mT (at the edge of the cylinder) in the infinite-wire model, the application of a short voltage pulse can switch the magnetization. This is because the increased H_K ($\mu_0 H_K = 570$ mT) during the voltage-pulse application is higher than $H_{\rm Oe}$.

Next we discuss the switching properties of the proposed switching scheme at $T = 300$ K by analyzing the results of the numerical simulations. The time evolution of the Cartesian components of $\hat{\mathbf{m}}$ for a typical switching trajectory during the pulse are shown in Fig. 3(a). The values of $K_{\rm eff}^p$ and α are the same as in Fig. 2(f), $K_{\rm eff}^p = 400$ kJ/m^3 and $\alpha = 0.21$. During the pulse duration, m_z increases with the increase of time because the effective anisotropy constant is increased. The shapes of m_x and m_y are very similar to the cosine and sine functions, respectively, because $\hat{\mathbf{m}}$ precesses around the effective field, which is almost parallel to the z axis. Figure 3(b) shows the time evolution of

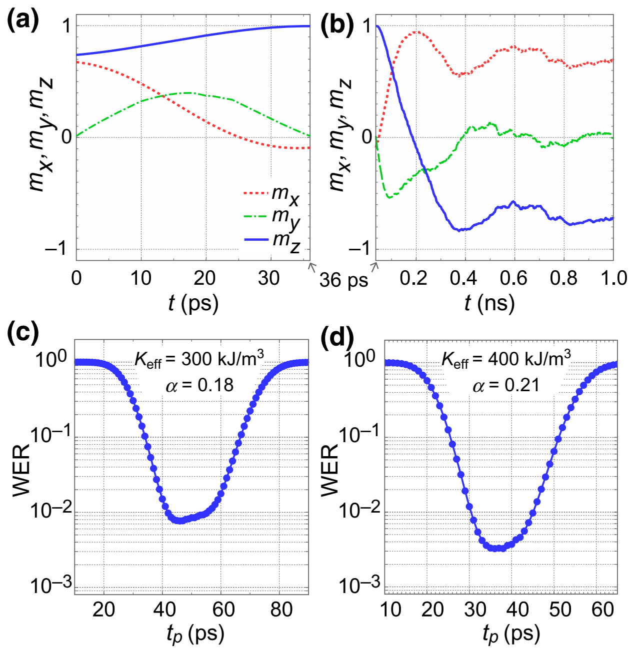

FIG. 3. (a) The Cartesian components of $\hat{\mathbf{m}} = (m_x, m_y, m_z)$ of a typical switching trajectory as a function of time during the pulse at $T = 300$ K. $K_{\mathrm{eff}}^p = 400$ kJ /m^3 and $\alpha = 0.21$. (b) The same as (a) after the pulse. (c) The pulse duration dependence of the WER at $T = 300$ K for $K_{\mathrm{eff}}^p = 300$ kJ /m^3 and $\alpha = 0.18$. (d) The same as (c) for $K_{\mathrm{eff}}^p = 400$ kJ /m^3 and $\alpha = 0.21$.

m_x, m_y, and m_z after the pulse. m_z monotonically decreases with the increase of time and the switching is completed at around 0.4 ns.

Figures 3(c) and 3(d) show the dependence of the WER on the pulse duration, t_p, for different values of K_{eff}^p and α. The values are $K_{\mathrm{eff}}^p = 300$ kJ /m^3 and $\alpha = 0.18$ for Fig. 3(c) and $K_{\mathrm{eff}}^p = 400$ kJ /m^3 and $\alpha = 0.21$ for Fig. 3(d). In Fig. 3(c), the WER has a minimum value of 7.6×10^{-3} at $t_p = 46$ ps. In Fig. 3(d), the WER has a minimum value of 3.2×10^{-3} at $t_p = 36$ ps. These optimal values of t_p at which the WER is minimized are almost the same as half the period of precession around H_{eff}.

In the simulation of the WER, we consider the macrospin model, zero-bias current, and the complete square voltage pulse without the pulse-rise time (t_r) and the pulse fall time (t_f) [37]. The inhomogeneity of the magnetization dynamics, however, causes the inhomogeneity of the precession period, and the WER should be greater than in the macrospin model. The STT induced by bias current density (J) of $|J| = 10^{12}$ A/m^2 with spin polarization of 0.6 in the macrospin simulation shown in Fig. 3(d) increases the WER by an order of magnitude, while the STT at $|J| \leq 10^{11}$ A/m^2 hardly affects the WER [39]. The macrospin simulations with t_r and t_f also result in an increase of the WER. With the introduction of $t_r = 10$ ps and $t_f = 10$ ps to the simulations shown in Fig. 3(d), the WER at $t_p = 36$ ps is 1.7×10^{-2}.

When the proposed writing scheme is applied out of the framework of approximate computing, some methods to reduce the WER are necessary. In this single-voltage-pulse switching scheme where the completion of switching relies on the relaxation of the magnetization to the lower-hemisphere equilibrium direction at $V = 0$, the increase of the thermal-stability factor and the in-plane external magnetic field should reduce the WER [38,40]. For further reduction of the WER, an additional short voltage pulse should be applied during the relaxation of the magnetization. However, the multiple-voltage-pulse switching scheme is beyond the scope of this letter.

In summary, we propose a low-power magnetization-switching scheme using enhanced magnetic anisotropy by applying a short voltage pulse. The proposed switching scheme can reduce the pulse duration and therefore the write energy substantially without reducing the thermal stability. We perform numerical simulations and show that the pulse duration of the proposed switching scheme is as short as a few tens of picoseconds. We also calculate the pulse duration dependence of the WER, and show that the optimal values of t_p at which the WER is minimized are nearly half period of precession around the effective field.

ACKNOWLEDGMENTS

This work was partly supported by JSPS KAKENHI Grants No. JP19K05259 and No. 19H01108.

[1] K. Ando, Nonvolatile magnetic memory, FED J. [in Japanese] **12**, 89 (2001).
[2] K. Ando, S. Fujita, J. Ito, S. Yuasa, Y. Suzuki, Y. Nakatani, T. Miyazaki, and H. Yoda, Spin-transfer torque magnetoresistive random-access memory technologies for normally off computing (invited), J. Appl. Phys. **115**, 172607 (2014).
[3] Takashi Nakada and Hiroshi Nakamura, eds., *Normally-Off Computing* (Springer, Tokyo, Japan, 2017).
[4] Shinji Yuasa, Taro Nagahama, Akio Fukushima, Yoshishige Suzuki, and Koji Ando, Giant room-temperature magnetoresistance in single-crystal Fe/MgO/Fe magnetic tunnel junctions, Nat. Mater. **3**, 868 (2004).
[5] Stuart S. P. Parkin, Christian Kaiser, Alex Panchula, Philip M. Rice, Brian Hughes, Mahesh Samant, and See-Hun Yang, Giant tunnelling magnetoresistance at room temperature with MgO (100) tunnel barriers, Nat. Mater. **3**, 862 (2004).
[6] David D. Djayaprawira, Koji Tsunekawa, Motonobu Nagai, Hiroki Maehara, Shinji Yamagata, Naoki Watanabe, Shinji Yuasa, Yoshishige Suzuki, and Koji Ando, 230% room-temperature magnetoresistance in CoFeB/MgO/CoFeB magnetic tunnel junctions, Appl. Phys. Lett. **86**, 092502 (2005).
[7] S. Yuasa and D. D. Djayaprawira, Giant tunnel magnetoresistance in magnetic tunnel junctions with a crystalline

MgO(0 0 1) barrier, J. Phys. D: Appl. Phys. **40**, R337 (2007).
[8] T. Kishi *et al.*, in *Proceedings of the IEEE International Electron Devices Meeting, San Francisco, 2008* (IEEE, New York, 2008).
[9] E. Kitagawa, S. Fujita, K. Nomura, H. Noguchi, K. Abe, K. Ikegami, T. Daibou, Y. Kato, C. Kamata, S. Kashiwada, N. Shimomura, J. Ito, and H. Yoda, in *Proceedings of the International Electron Devices Meeting, San Francisco, 2012* (IEEE, New York, 2012), p. 29.4.1.
[10] Dmytro Apalkov, Bernard Dieny, and J. M. Slaughter, Magnetoresistive random access memory, Proc. IEEE **104**, 1796 (2016).
[11] Rachid Sbiaa and S. N. Piramanayagam, Recent developments in spin transfer torque MRAM, Phys. Status Solidi (RRL) – Rapid Res. Lett. **11**, 1700163 (2017).
[12] Hao Cai, Wang Kang, You Wang, Lirida Alves De Barros Naviner, Jun Yang, and Weisheng Zhao, High performance MRAM with spin-transfer-torque and voltage-controlled magnetic anisotropy effects, Appl. Sci. **7**, 929 (2017).
[13] J. C. Slonczewski, Conductance and exchange coupling of two ferromagnets separated by a tunneling barrier, Phys. Rev. B **39**, 6995 (1989).
[14] J. C. Slonczewski, Current-driven excitation of magnetic multilayers, J. Magn. Magn. Mater. **159**, L1 (1996).
[15] L. Berger, Emission of spin waves by a magnetic multilayer traversed by a current, Phys. Rev. B **54**, 9353 (1996).
[16] Martin Weisheit, Sebastian Fähler, Alain Marty, Yves Souche, Christiane Poinsignon, and Dominique Givord, Electric field-induced modification of magnetism in thin-film ferromagnets, Science **315**, 349 (2007).
[17] T. Maruyama, Y. Shiota, T. Nozaki, K. Ohta, N. Toda, M. Mizuguchi, A. A. Tulapurkar, T. Shinjo, M. Shiraishi, S. Mizukami, Y. Ando, and Y. Suzuki, Large voltage-induced magnetic anisotropy change in a few atomic layers of iron, Nat. Nano. **4**, 158 (2009).
[18] Chun-Gang Duan, Julian P. Velev, R. F. Sabirianov, Ziqiang Zhu, Junhao Chu, S. S. Jaswal, and E. Y. Tsymbal, Surface Magnetoelectric Effect in Ferromagnetic Metal Films, Phys. Rev. Lett. **101**, 137201 (2008).
[19] Kohji Nakamura, Riki Shimabukuro, Yuji Fujiwara, Toru Akiyama, Tomonori Ito, and A. J. Freeman, Giant Modification of the Magnetocrystalline Anisotropy in Transition-Metal Monolayers by an External Electric Field, Phys. Rev. Lett. **102**, 187201 (2009).
[20] Masahito Tsujikawa and Tatsuki Oda, Finite Electric Field Effects in the Large Perpendicular Magnetic Anisotropy Surface Pt/Fe/Pt(001): A First-Principles Study, Phys. Rev. Lett. **102**, 247203 (2009).
[21] T. Nozaki, Y. Shiota, M. Shiraishi, T. Shinjo, and Y. Suzuki, Voltage-induced perpendicular magnetic anisotropy change in magnetic tunnel junctions, Appl. Phys. Lett. **96**, 022506 (2010).
[22] M. Endo, S. Kanai, S. Ikeda, F. Matsukura, and H. Ohno, Electric-field effects on thickness dependent magnetic anisotropy of sputtered $MgO/Co_{40}Fe_{40}B_{2}0/Ta$ structures, Appl. Phys. Lett. **96**, 212503 (2010).
[23] Takayuki Nozaki, Hiroko Arai, Kay Yakushiji, Shingo Tamaru, Hitoshi Kubota, Hiroshi Imamura, Akio Fukushima, and Shinji Yuasa, Magnetization switching assisted by high-frequency-voltage-induced ferromagnetic resonance, Appl. Phys. Express **7**, 073002 (2014).
[24] Witold Skowroński, Takayuki Nozaki, Yoichi Shiota, Shingo Tamaru, Yakushiji Kay, Hitoshi Kubota, Akio Fukushima, Shinji Yuasa, and Yoshishige Suzuki, Perpendicular magnetic anisotropy of Ir/CoFeB/MgO trilayer system tuned by electric fields, Appl. Phys. Express **8**, 053003 (2015).
[25] Takayuki Nozaki, Anna Kozioł-Rachwał, Witold Skowroński, Vadym Zayets, Yoichi Shiota, Shingo Tamaru, Hitoshi Kubota, Akio Fukushima, Shinji Yuasa, and Yoshishige Suzuki, Large Voltage-Induced Changes in the Perpendicular Magnetic Anisotropy of an MgO-Based Tunnel Junction with an Ultrathin Fe Layer, Phys. Rev. Appl. **5**, 044006 (2016).
[26] Xiang Li, Kevin Fitzell, Di Wu, C. Ty Karaba, Abraham Buditama, Guoqiang Yu, Kin L. Wong, Nicholas Altieri, Cecile Grezes, Nicholas Kioussis, Sarah Tolbert, Zongzhi Zhang, Jane P. Chang, Pedram Khalili Amiri, and Kang L. Wang, Enhancement of voltage-controlled magnetic anisotropy through precise control of Mg insertion thickness at CoFeB—MgO interface, Appl. Phys. Lett. **110**, 052401 (2017).
[27] Shinji Miwa, Motohiro Suzuki, Masahito Tsujikawa, Kensho Matsuda, Takayuki Nozaki, Kazuhito Tanaka, Takuya Tsukahara, Kohei Nawaoka, Minori Goto, Yoshinori Kotani, Tadakatsu Ohkubo, Frédéric Bonell, Eiiti Tamura, Kazuhiro Hono, Tetsuya Nakamura, Masafumi Shirai, Shinji Yuasa, and Yoshishige Suzuki, Voltage controlled interfacial magnetism through platinum orbits, Nat. Commun. **8**, 15848 (2017).
[28] Yoichi Shiota, Takayuki Nozaki, Frédéric Bonell, Shinichi Murakami, Teruya Shinjo, and Yoshishige Suzuki, Induction of coherent magnetization switching in a few atomic layers of FeCo using voltage pulses, Nat. Mater. **11**, 39 (2012).
[29] Yoichi Shiota, Shinji Miwa, Takayuki Nozaki, Frédéric Bonell, Norikazu Mizuochi, Teruya Shinjo, Hitoshi Kubota, Shinji Yuasa, and Yoshishige Suzuki, Pulse voltage-induced dynamic magnetization switching in magnetic tunneling junctions with high resistance-area product, Appl. Phys. Lett. **101**, 102406 (2012).
[30] S. Kanai, M. Yamanouchi, S. Ikeda, Y. Nakatani, F. Matsukura, and H. Ohno, Electric field-induced magnetization reversal in a perpendicular-anisotropy CoFeB-MgO magnetic tunnel junction, Appl. Phys. Lett. **101**, 122403 (2012).
[31] Yoichi Shiota, Takayuki Nozaki, Shingo Tamaru, Kay Yakushiji, Hitoshi Kubota, Akio Fukushima, Shinji Yuasa, and Yoshishige Suzuki, Evaluation of write error rate for voltage-driven dynamic magnetization switching in magnetic tunnel junctions with perpendicular magnetization, Appl. Phys. Express **9**, 013001 (2016).
[32] C. Grezes, F. Ebrahimi, J. G. Alzate, X. Cai, J. A. Katine, J. Langer, B. Ocker, P. Khalili Amiri, and K. L. Wang, Ultra-low switching energy and scaling in electric-field-controlled nanoscale magnetic tunnel junctions with high resistance-area product, Appl. Phys. Lett. **108**, 012403 (2016).
[33] S. Kanai, F. Matsukura, and H. Ohno, Electric-field-induced magnetization switching in CoFeB/MgO magnetic

tunnel junctions with high junction resistance, Appl. Phys. Lett. **108**, 192406 (2016).

[34] Yoichi Shiota, Takayuki Nozaki, Shingo Tamaru, Kay Yakushiji, Hitoshi Kubota, Akio Fukushima, Shinji Yuasa, and Yoshishige Suzuki, Reduction in write error rate of voltage-driven dynamic magnetization switching by improving thermal stability factor, Appl. Phys. Lett. **111**, 022408 (2017).

[35] R. Matsumoto, T. Nozaki, S. Yuasa, and H. Imamura, Voltage-Induced Precessional Switching at Zero-Bias Magnetic Field in a Conically Magnetized Free Layer, Phys. Rev. Appl. **9**, 014026 (2018).

[36] Tatsuya Yamamoto, Takayuki Nozaki, Yoichi Shiota, Hiroshi Imamura, Shingo Tamaru, Kay Yakushiji, Hitoshi Kubota, Akio Fukushima, Yoshishige Suzuki, and Shinji Yuasa, Thermally Induced Precession-Orbit Transition of Magnetization in Voltage-Driven Magnetization Switching, Phys. Rev. Appl. **10**, 024004 (2018).

[37] Tatsuya Yamamoto, Takayuki Nozaki, Hiroshi Imamura, Yoichi Shiota, Takuro Ikeura, Shingo Tamaru, Kay Yakushiji, Hitoshi Kubota, Akio Fukushima, Yoshishige Suzuki, and Shinji Yuasa, Write-Error Reduction of Voltage-Torque-Driven Magnetization Switching by a Controlled Voltage Pulse, Phys. Rev. Appl. **11**, 014013 (2019).

[38] Rie Matsumoto, Tomoyuki Sato, and Hiroshi Imamura, Voltage-induced switching with long tolerance of voltage-pulse duration in a perpendicularly magnetized free layer, Appl. Phys. Express **12**, 053003 (2019).

[39] Hiroshi Imamura and Rie Matsumoto, Impact of Spin-Transfer Torque on the Write-Error Rate of a Voltage-Torque-Based Magnetoresistive Random-Access Memory, Phys. Rev. Appl. **11**, 064019 (2019).

[40] R. Matsumoto and H. Imamura, Methods for reducing write error rate in voltage-induced switching having prolonged tolerance of voltage-pulse duration, AIP Adv. **9**, 125123 (2019).

[41] William Fuller Brown, Thermal fluctuations of a single-domain particle, Phys. Rev. **130**, 1677 (1963).

[42] Arne Vansteenkiste, Jonathan Leliaert, Mykola Dvornik, Mathias Helsen, Felipe Garcia-Sanchez, and Bartel Van Waeyenberge, The design and verification of MuMax3, AIP Adv. **4**, 107133 (2014).